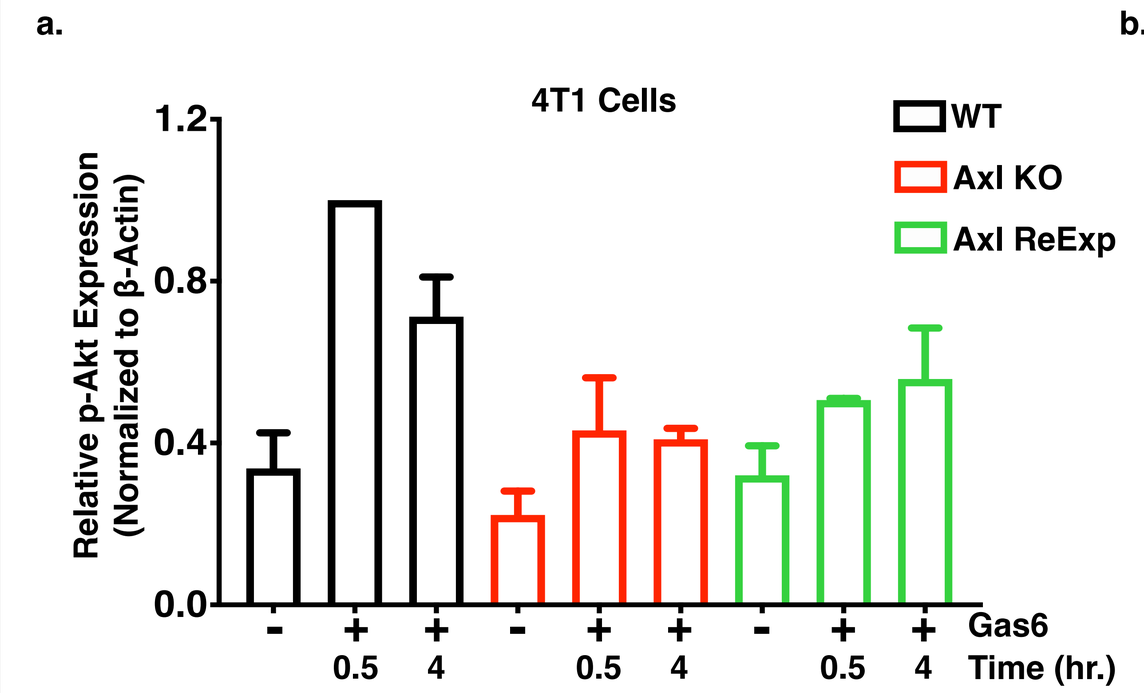

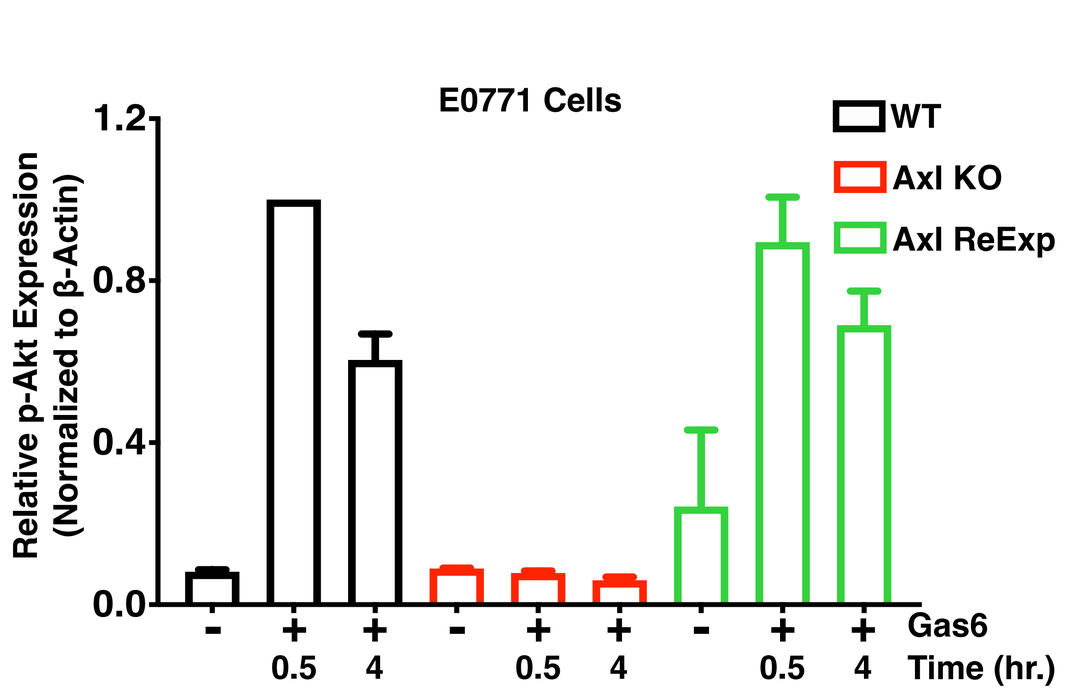

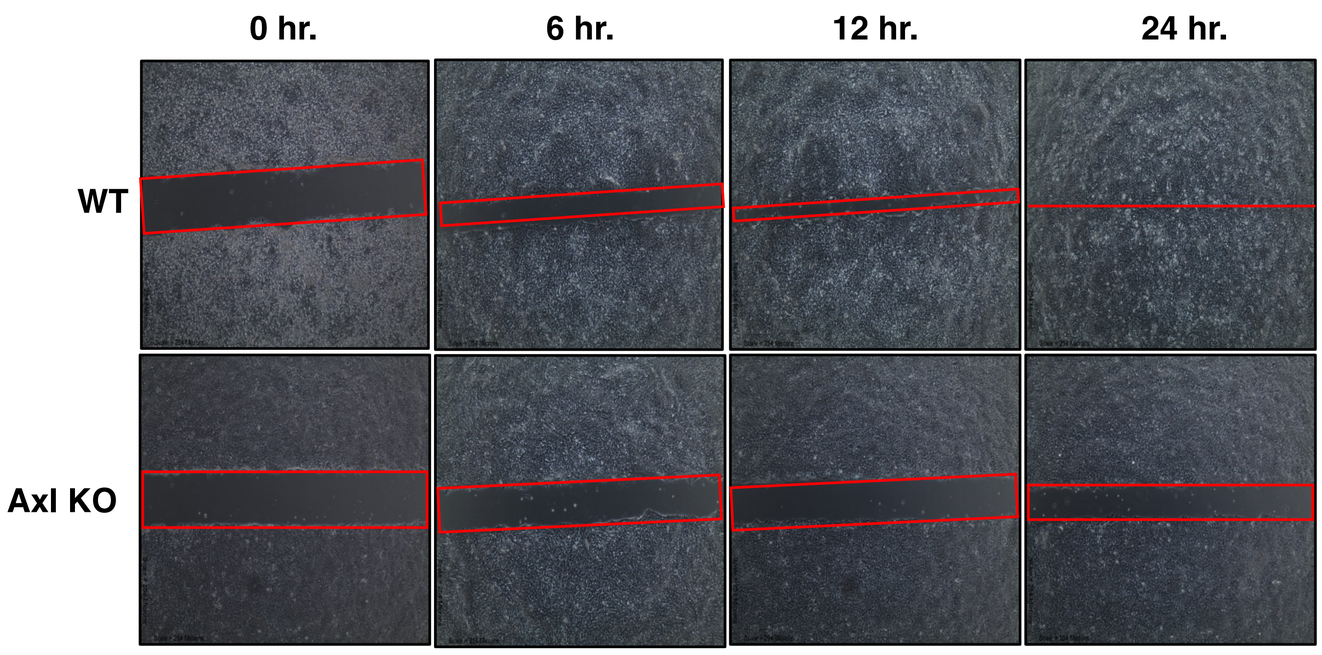

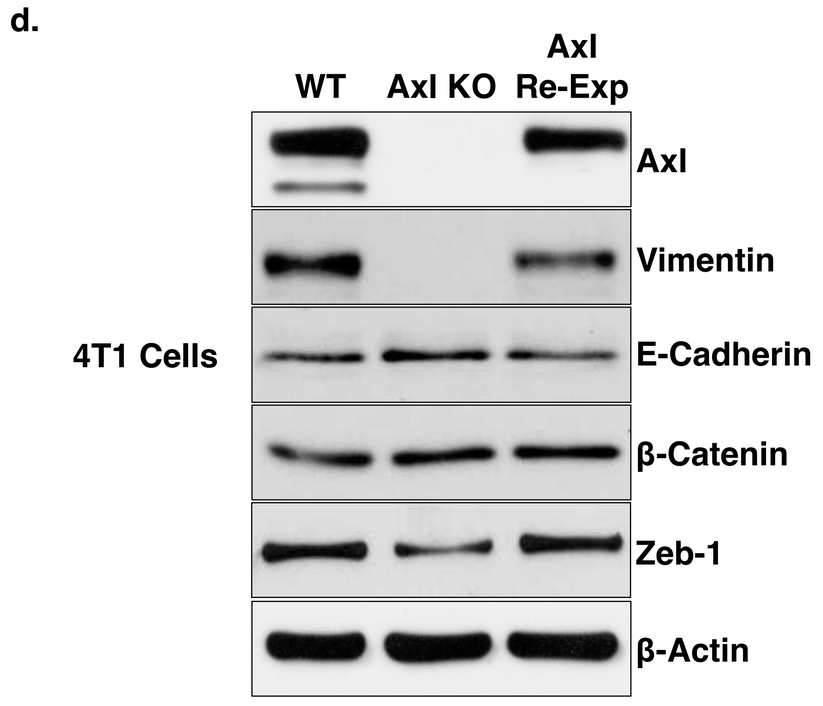

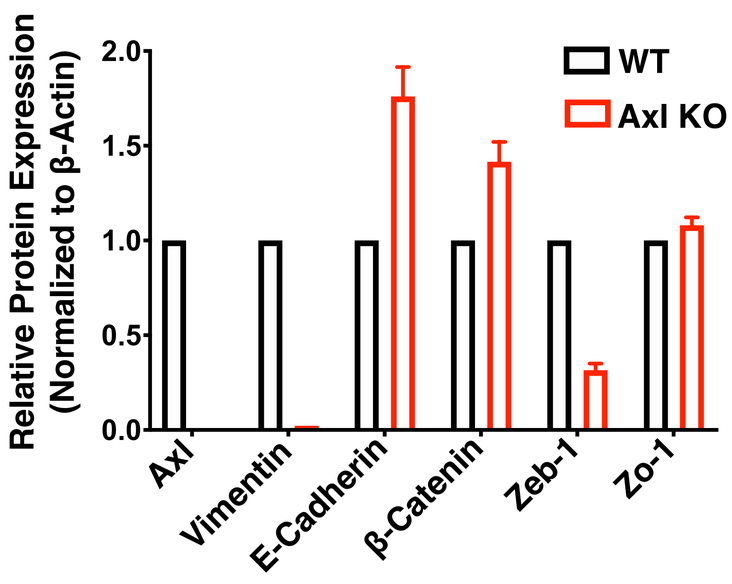

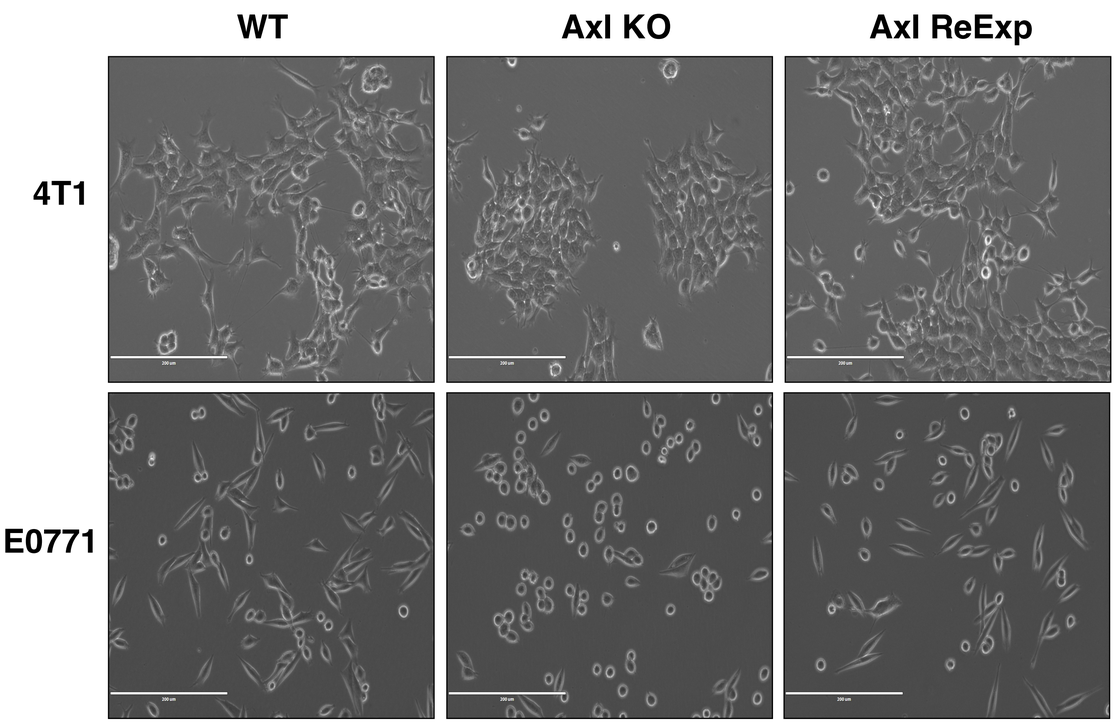

Fig. S1. Effect of Axl receptor genetic deletion on cell intrinsic tumorigenic properties. a-b. Bargraph showing normalized expression of phospho Akt immunoblots from 4T1 **(a)** and E0771 **(b)-** WT, Axl KO and Axl Re-Exp. cells treated with ligand, Gas6, for 30 mins and 4 hrs., in the 4T1 and E0771- WT, Axl KO and Axl Re-Exp. cells **c.** Cell migration of the 4T1-Wt and Axl receptor KO as determined by wound healing assay. **d.** Immunoblots depicting EMT markers in 4T1- WT, Axl KO and Axl Re-Exp. **e.** cells Bar-graph analysis showing normalized expression of EMT markers immunoblots to β-Actin in from 4T1-Wt and Axl KO cells. **f.** Representative images depecting 4T1 and E0771- WT, Axl KO and Axl Re-Exp. cells morphology.

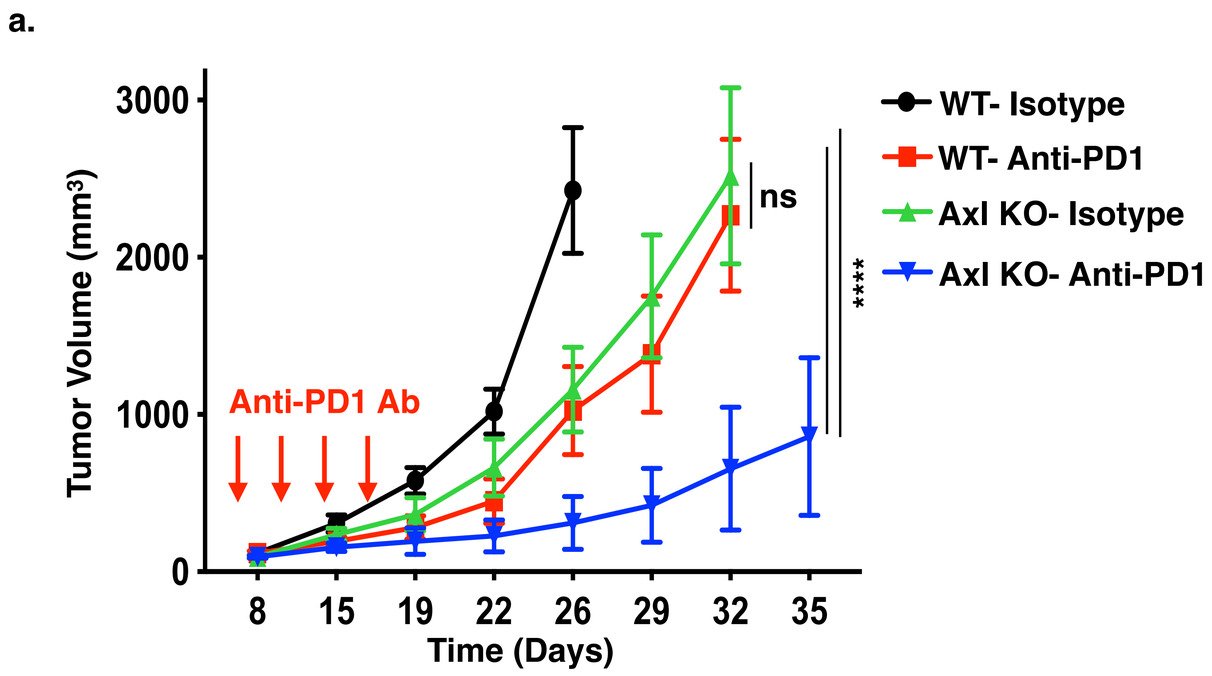

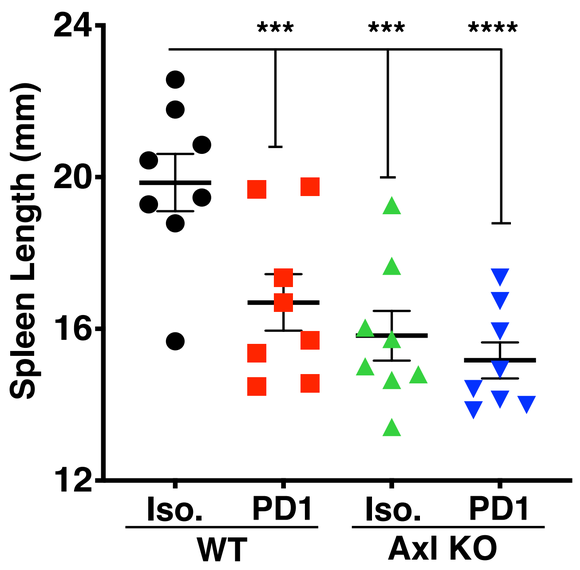

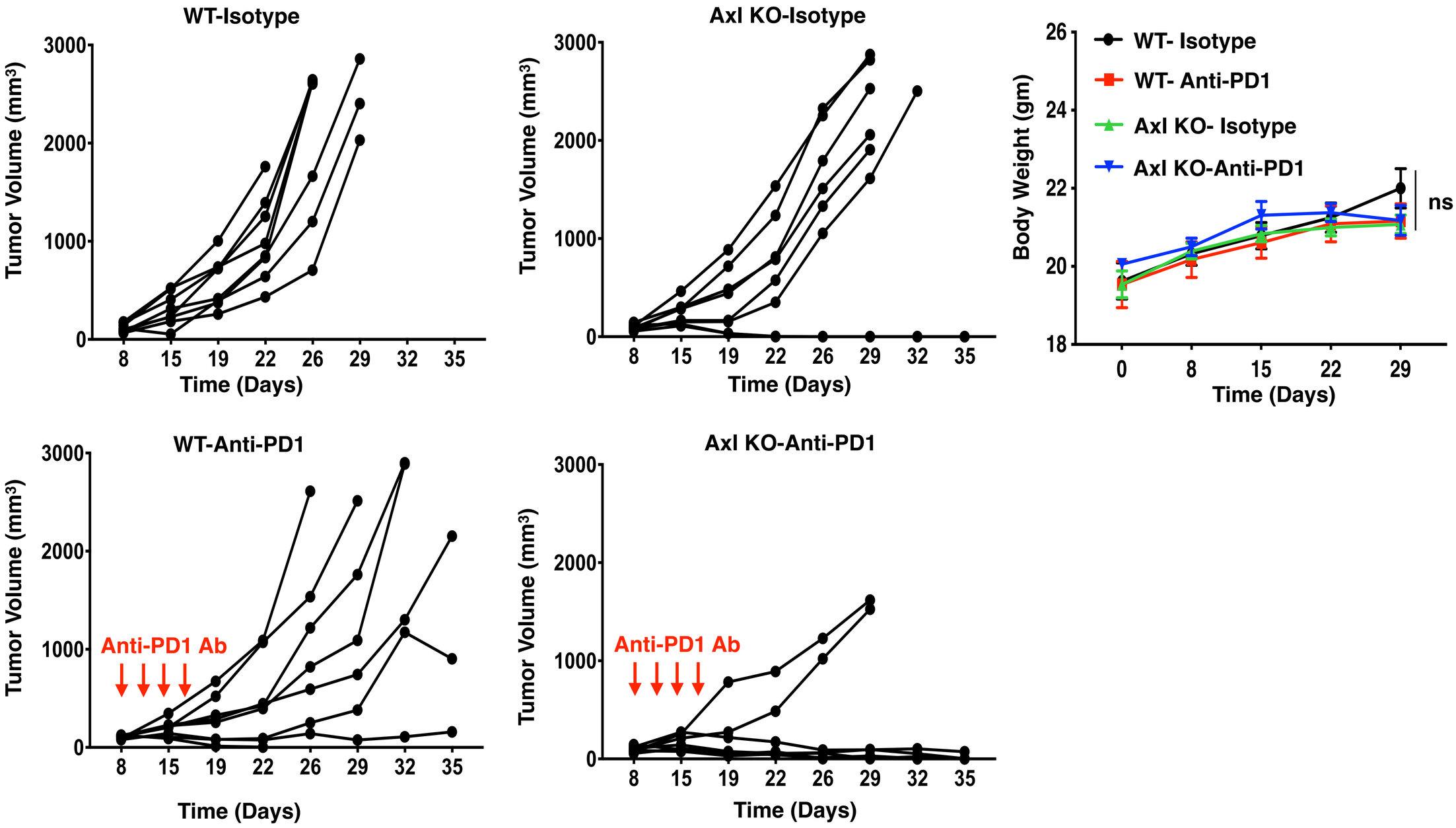

Fig. S2. Genetic deletion of Axl receptor in murine breast cancer cells inhibit tumor growth and synergies with anti-PD1 immunotherapy in the preclinical murine breast cancer model. a. Tumor growth analysis of E0771-WT and Axl KO tumor bearing mice (n=8/group) treated with mIgG1 Isotype control Ab or anti-PD1 Ab (5 mg/kg) on day 6, 9, 12, and 15. Arrows indicate antibody injections. **b.** Spider curve showing tumor growth analysis in the E0771-WT and Axl KO tumor bearing mice (n=8/group) treated with mIgG1 Isotype control Ab or anti-PD1 Ab. **c.** Upon sacrifice, spleens were also collected, and their length were quantified. **d.** The whole-body weight of mice was measured once a week over the period of 4 weeks

Supp. Fig. 2

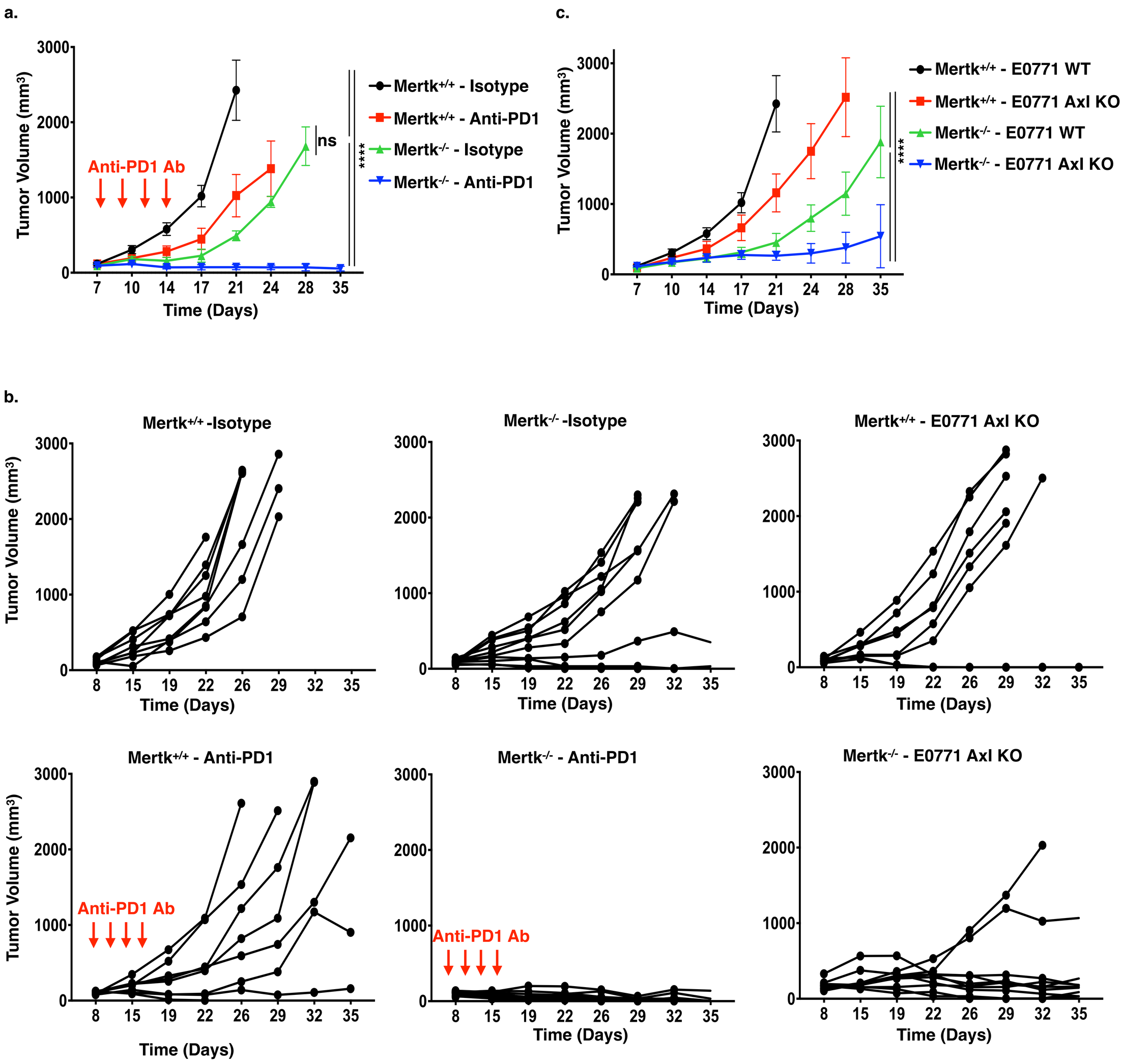

Figure S3. Mertk deficiency decreases tumor malignancy and synergize with anti-PD1 immunotherapy in the E0771 murine breast cancer model. a. Tumor growth analysis of E0771-WT tumor cells injected orthotopically in to the mammary fat pad of female c57BL/6- Mertk$^{+/+}$ (WT) and Mertk$^{-/-}$ (Mertk KO) mice, and upon establishment of tumors, mice were treated with mIgG1 Isotype or anti-PD1 antibody (5 mg/kg) on day 6, 9, 12, and 15 and tumor growth determined by means tumor volume measurement every 3 days over the period of 5 weeks. (n=8/per group). **b.** Spider curve showing tumor growth analysis in the different treatment groups in Mertk$^{+/+}$ and Mertk$^{-/-}$ mice. **c.** Tumor growth analysis of E0771-WT and Axl KO tumor cells injected orthotopically in to the mammary fat pad of female c57BL/6- Mertk$^{+/+}$ and Mertk$^{-/-}$ mice.

a.

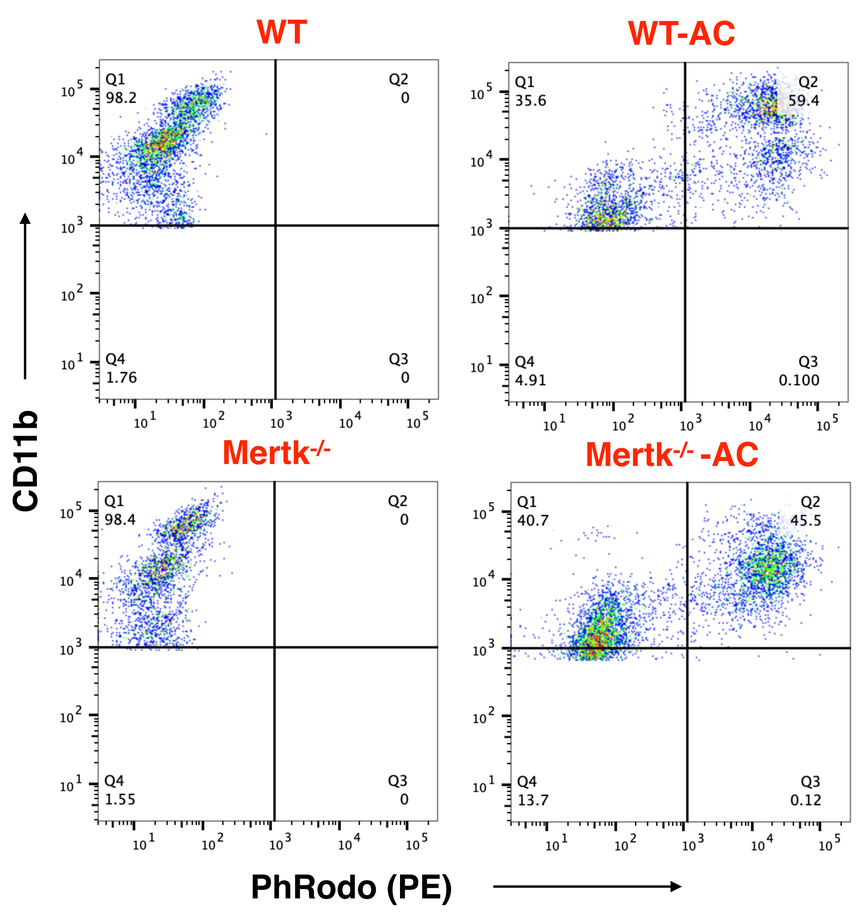

b.

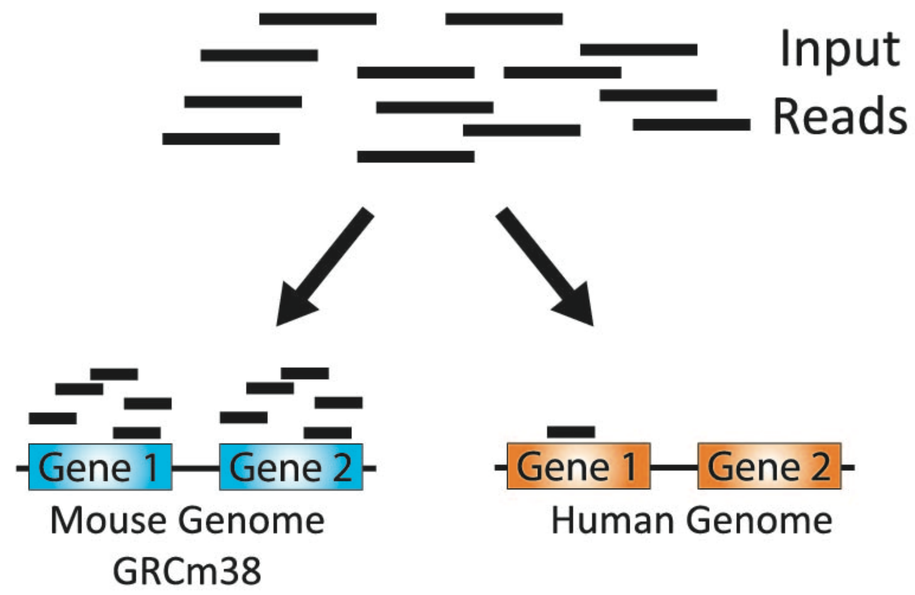

c.

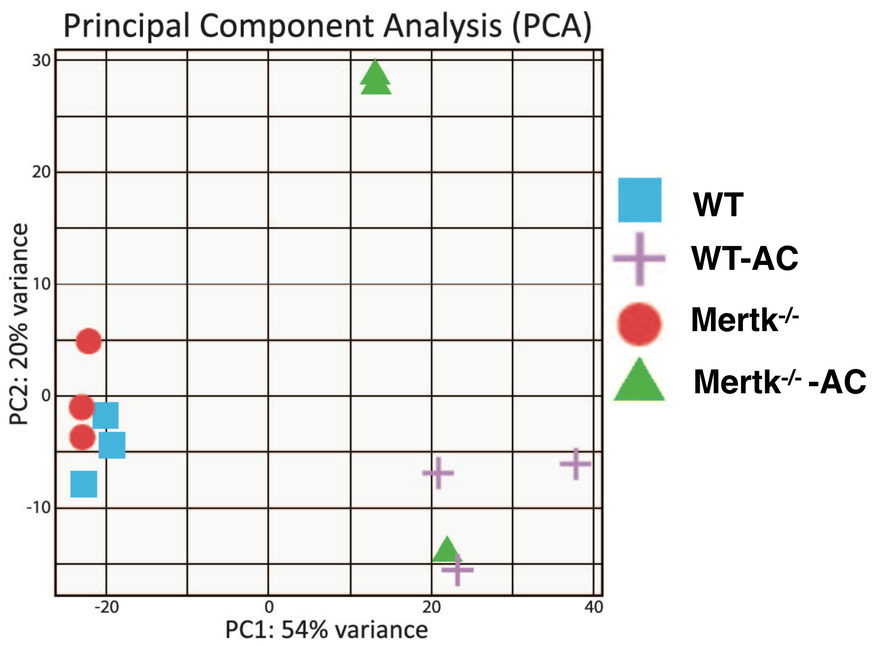

d.

Genes	WT vs Mertk$^{-/-}$	WT vs WT-AC	Mertk$^{-/-}$ vs Mertk$^{-/-}$ -AC	WT-AC vs Mertk$^{-/-}$ -AC
PTGS2	-6.2549	286.6857	116.4315	-15.4013
CCL4	-2.0185	45.4427	31.7524	-2.8888
Ccl2	1.2189	38.3227	16.9757	-1.8520
CCL3L3	-2.2493	25.2512	21.5348	-2.6374
CXCL10	-2.6436	10.3995	7.9612	-3.4532
CSF3	-4.9760	349.6706	93.6750	-18.5743
IL10	-2.1048	110.5470	41.9003	-5.5532
TNF	-1.4015	73.0761	23.8129	-4.3009
CD44	-1.4898	2.0928	1.8510	-1.6845
ADORA2B	1.0505	5.4627	2.8883	-1.8003
ITGA5	1.1494	4.6671	2.2580	-1.7983
CX3CR1	-1.1353	-1.9949	-3.5775	-2.0360
IL1B	-2.6704	73.9118	11.3352	-17.4126
IL6	-2.0445	17.8515	4.4711	-8.1630
PLEC	1.3709	3.3053	1.2790	-1.8852
C3	-1.2302	1.4840	1.1449	-1.5946
Retnla	1.4747	-1.3719	3.1318	6.3363
LRRK2	-1.3792	1.6006	-1.0725	-2.3675
HCK	-1.5624	1.1840	1.0057	-1.8393

Fig. S4. Effect of Mertk receptor ablation on the efferocytosis mediated gene expression profile. **a.** Flowcytometry analysis showing CD11b F4/80 positive macrophages with engulfed apoptotic cells in WT vs Mertk deficient macrophages. **b.** Model depicting approach used for consideration of the homology between human and mouse genome, resulting in a proportion of human reads being segregated from mouse. A thorough investigation on potential cross-mapping was performed. **c.** Principal component analysis showing variance among the experimental samples. **d.** Fold change data demonstrated among the genes selected from inflammatory response and activation of macrophages pathways from ingenuity pathway analysis.

Supp. Fig. 4

a.

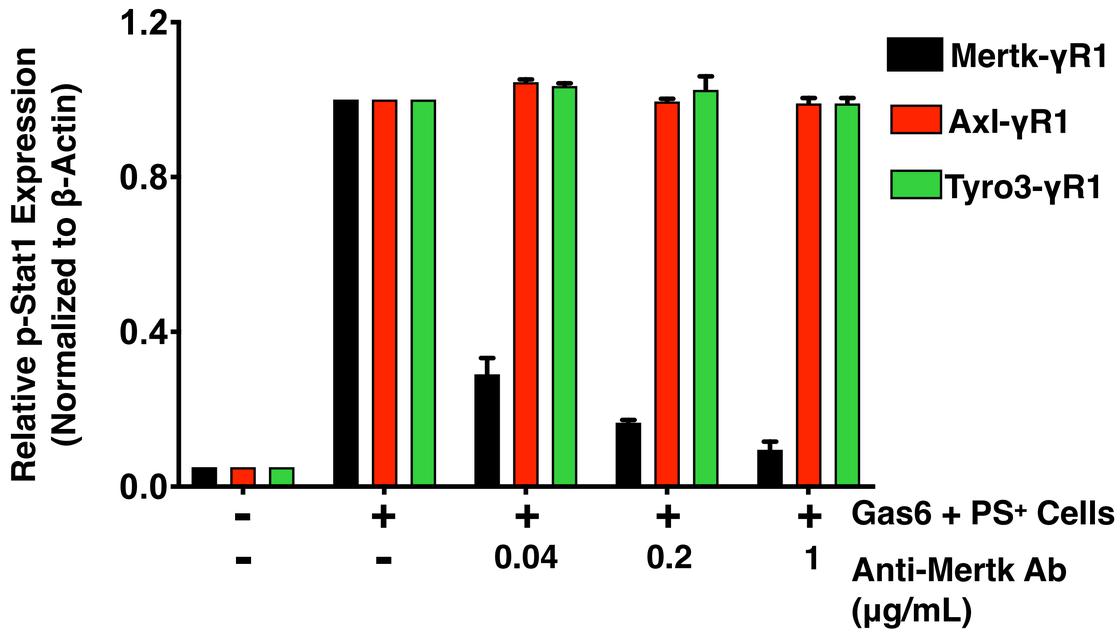

b.

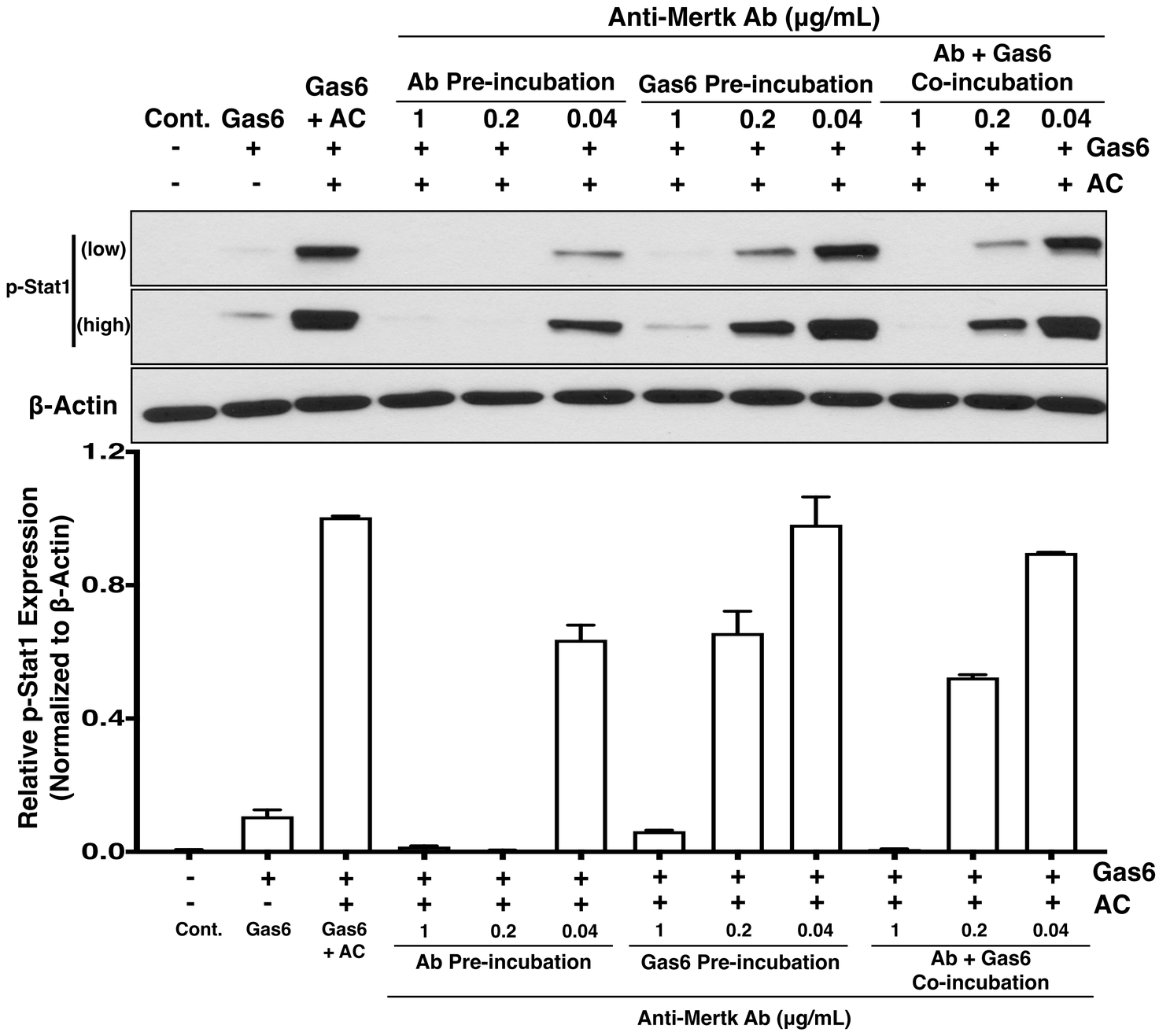

Fig. S5. Effect of Anti-mertk ab on the Mertk receptor inhibition. a. Bargraph showing normalized expression of phospho Stat1 immunoblots from Mertk-γR1, Axl-γR1, Tyro3-γR1 cells pretreated with anti-Mertk antibody followed by Gas6 and apoptotic cells treatement for 30 mins **b.** Immunoblot analysis showing anti-Mertk antibody induced inhibition of Gas6 and apoptotic cells mediated activation of Mertk receptors in the CHO cells expressing chimeric murine Mer-γR1 receptors.

Supp. Fig. 5

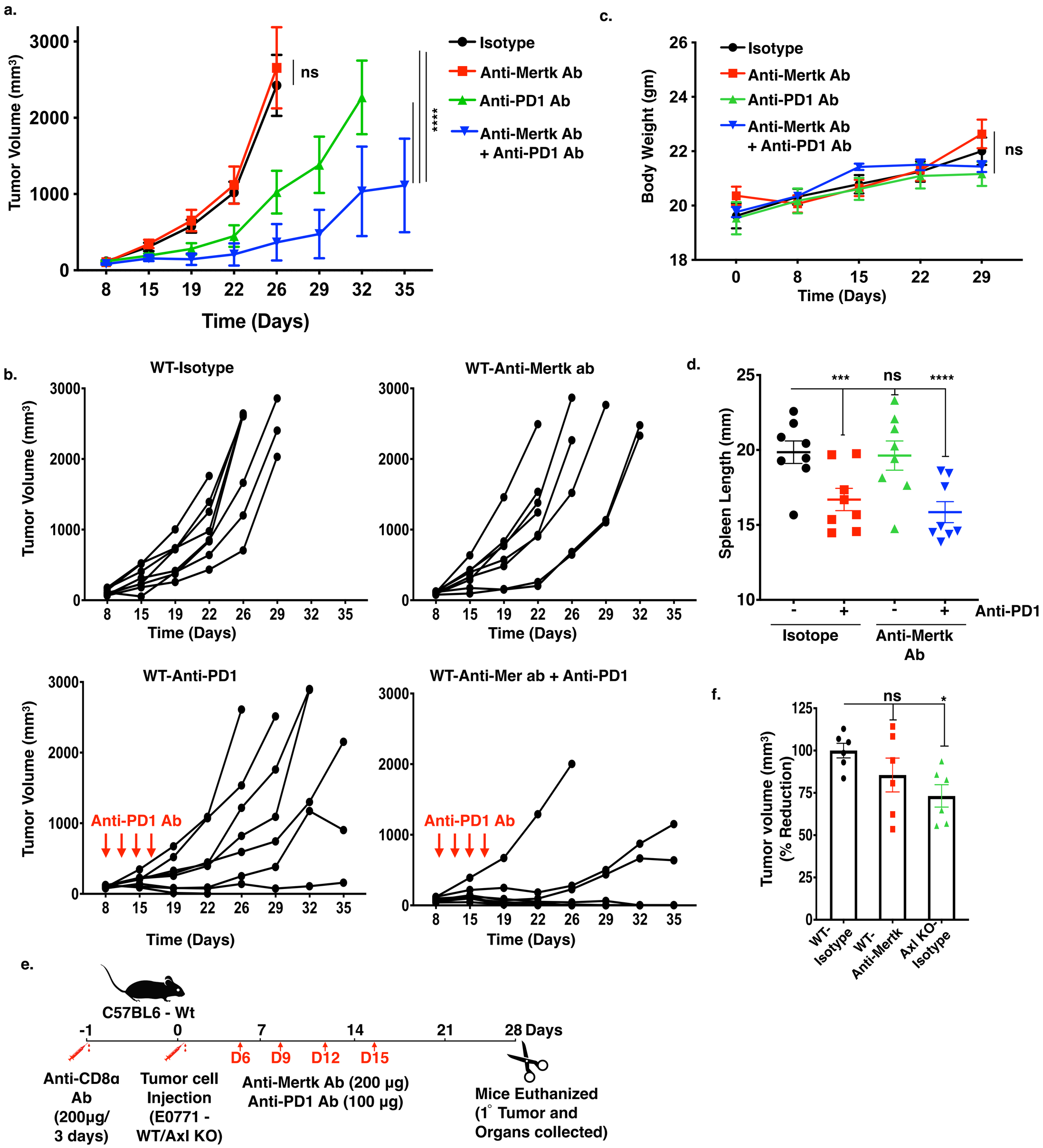

Fig. S6. Effect of Anti-mertk ab on the Mertk receptor inhibition on tumor growth. a. Anti-tumor effect of anti-Mertk mAb in combination with Anti-PD1 immunotherapy. E0771 tumor bearing females C57/B16 (n=8/per group) were treated with mIgG1 Isotype control, anti-Mertk aAb (10mg/kg), anti-PD1 ab (5mg/Kg) alone and anti-Mertk ab in combination with anti-PD1 ab on day 6, 9,12, and15 and tumor growth was studied twice a week over the period of 4 weeks. **b.** Spider curve showing tumor growth analysis in E0771 tumor bearing females C57/B16 (n=8/per group) treated with mIgG1 Isotype control, anti-Mertk aAb (10mg/kg), anti-PD1 ab (5mg/Kg) alone and anti-Mertk ab in combination with anti-PD1 ab. **c.** The whole-body weight of mice was measured once a week over the period of 4 weeks. **d.** Upon sacrifice, spleens were also collected, and splenomegaly was quantified by means of spleen Length. **e.** Experimental mouse model depicting Anti-CD8α ab treatment regimen in the mice injected with E0771 WT or Axl KO tumor cells or injected with E0771 WT cells and treated with anti-Mertk Ab alone or in combination with anti-PD1 immunotherapy. **f.** Bar graph representing tumor growth at d28 from the individual mice from each group from SCID mice.

Supp. Fig. 6